



## Accurate corner detection : an analytical study

Rachid Deriche, Gerard Giraudon

### ► To cite this version:

Rachid Deriche, Gerard Giraudon. Accurate corner detection : an analytical study. [Research Report] RR-1420, INRIA. 1991, pp.42. inria-00075140

**HAL Id: inria-00075140**

**<https://inria.hal.science/inria-00075140>**

Submitted on 24 May 2006

**HAL** is a multi-disciplinary open access archive for the deposit and dissemination of scientific research documents, whether they are published or not. The documents may come from teaching and research institutions in France or abroad, or from public or private research centers.

L'archive ouverte pluridisciplinaire **HAL**, est destinée au dépôt et à la diffusion de documents scientifiques de niveau recherche, publiés ou non, émanant des établissements d'enseignement et de recherche français ou étrangers, des laboratoires publics ou privés.



UNITÉ DE RECHERCHE  
IRIA-SOPHIA ANTIPOLIS

# Rapports de Recherche

N° 1420

*Programme 4*  
*Robotique, Image et Vision*

## ACCURATE CORNER DETECTION : AN ANALYTICAL STUDY

Institut National  
de Recherche  
en Informatique  
et en Automatique

Domaine de Voluceau  
Rocquencourt  
B.P. 105  
78153 Le Chesnay Cedex  
France  
Tél. (1) 39 63 55 11

Rachid DERICHE  
Gérard GIRAUDON

Avril 1991



# Accurate Corner Detection : An Analytical Study <sup>1</sup>

## Extraction précise de points anguleux : Une étude analytique

Rachid DERICHE and Gerard GIRAUDON

INRIA 2004 Route des Lucioles - Sophia Antipolis

0650 VALBONNE - FRANCE

April 1991

*Programme 4: Robotique, Image et Vision*

---

<sup>1</sup>This work has been partially made under PRC *Orasis* contract and Esprit Project P2502 *Voila*.

### **Abstract**

Corners are often used in Computer Vision for scene analysis, stereo matching or motion analysis. In this paper, we consider a corner model and study analytically its behaviour in the scale-space. We derive results that clarify completely the behaviour of some well known approaches used to detect corners. In particular, we will show that some of them are inadequate for an exact localization of the corner. We propose a new approach that will allow to detect exactly the corner position and some promising experimental results on real data will be shown.

### **Résumé**

La caractérisation et la localisation des coins dans une image sont très utiles en Vision par Ordinateur que ce soit pour l'analyse de scène, pour la mise en correspondance stéréo ou bien encore pour l'analyse du mouvement. Dans ce rapport, nous établissons le modèle d'un coin et nous étudions analytiquement son comportement dans l'espace des échelles. Cela nous permet d'obtenir des résultats qui clarifient complètement le comportement des approches bien connues dans la littérature pour la détection des coins. En particulier, nous montrons que l'utilisation de certaines de ces approches entraînent une erreur pouvant être importante sur la localisation du coin. Aussi, nous proposons une nouvelle approche qui permet de pallier à ce type de défauts. Nous montrons quelques résultats expérimentaux sur des images synthétiques et sur des scènes réelles, qui démontrent l'intérêt et la justesse de la méthode.

## 1 Introduction

In scene analysis, the goal of low level vision is image segmentation, in particular feature extraction. One of the most popular technique is edge extraction. An expansive literature has been developed from Marr and Hildreth's works [Mar80] to Canny or Deriche's works [Can86], [Der87] based on the first or second derivatives of images. These works use an Heaviside function to modelize a step edge. This model, essentially one-dimensional, cannot give access directly to another class of important features in scene analysis: corners. To obtain these features from edges, line segments from polygonal approximation or curvature analysis along edge chains must be used [Asa86], [Der88], [Med86].

Corner detection is very important because this feature represents a relevant information in computer vision. Corners are often used to identify objects in the scene or used for stereoscopic matching or displacement vector measuring etc... So, accurate localization of corner detection is of great interest.

An alternative method can be used to detect corners directly from a gray-level image. So, several techniques have been proposed in this way. These techniques are based either on heuristics like the "interest operator" of Moravec [Mor77] or on the measurement of the gradients and of the curvatures of the surface. In this second type, we find works of Dreschler and Nagel [Dre82], [Nag83a], Kitchen and Rosenfeld [Kit82] and more recently works of Noble [Nob88] Harris and Stephen [Har88] and Guiducci [Gui88].

In this paper which deals with the second type of approach, we present an analytical study of some classical operators and "cornerness" measurement in the vicinity of the point of interest. The main characteristic of this paper is to give a formal representation of corner detection. In particular, this study allows us to know exactly what is the behavior of some classical measures like the one proposed by Nagel or Kitchen and to correct their faulty localization. This analytical study gives the real corner point and an implementation is proposed to find this point exactly. Some experimental results on real scenes will be shown.

The paper is organized as follows. A first section is devoted to the presentation of previous works in corner detection. In the second section, we present the analytical study that deals with the corner detection problem, and allows us to better understand what happens around such points of interest. A last section is then devoted to the application of this analytical study. Some experimental and promising results will illustrate this part. An appendix gives some elementary results of surface differential geometry that are used in the paper.

## 2 Previous Works

In this section, we briefly review some classical corner detector presented in the literature. Our review is neither intended to be exhaustive nor does it aim to present corner detectors in detail. Several approaches to the problem of detecting feature points have been reported in the literature in the last few years. They can be broadly divided into two groups.

The first group involves first extracting edges as a chain code and then searching for points having maxima curvature. Maxima curvature points can be found as following :

- At every chain code point, the unit vector tangent is estimated by using pixel coordinates of chain code (see [Asa86], [Med86] or [Mok86])
- At every chain code point, the unit vector tangent is estimated by using the partial derivatives of image  $I(x, y)$  with respect to  $x$  and  $y$  (see [Der88]).

The second group consists of approaches that work directly at the gray scale level. Gray scale level based corner detectors are then used to compute locally a measure of *cornerness*  $C$  defined as the product of gradient magnitude and the rate of change of gradient direction. Corners are then obtained by thresholding. Among the most popular corner detectors are those proposed by : Beaudet [Bea78], Dreschler and Nagel [Dre82], Kitchen and Rosenfeld [Kit82], and Zuniga and Haralick [Zun83]. In fact, it has been reported by Nagel [Nag83a] and by Shah and Jain [Sha84] that the three last detectors are equivalent. A more recent approach is the one developed by Harris and Stephens [Har88] and Noble [Nob88]

In 1978, Beaudet [Bea78] proposed a rotationally invariant operator called DET derived using a second order Taylors's expansion of the intensity surface  $I(x, y)$  :

$$DET = I_{xx}I_{yy} - I_{xy}^2 \quad (1)$$

The corner detection is based on the thresholding of the absolute value of the extrema of this operator.

In fact, this operator can be interpreted as the **Hessian** determinant,

$$\mathbf{H} = \begin{bmatrix} I_{xx} & I_{xy} \\ I_{yx} & I_{yy} \end{bmatrix} \quad (2)$$

which is related to the product of the principal curvatures  $\kappa_{min}$   $\kappa_{max}$ , called the Gaussian Curvature [Lip69] as follows :

$$(\kappa_{min}\kappa_{max}) = \frac{DET}{(1 + I_x^2 + I_y^2)^2} \quad (3)$$

In terms of differential geometry, we can say : for a pixel  $I(x, y)$ ,

If  $\kappa_{min}\kappa_{max} > 0 \iff$  the pixel is an elliptic point

If  $\kappa_{min}\kappa_{max} < 0 \iff$  the pixel is a hyperbolic point

If  $\kappa_{min}\kappa_{max} = 0 \iff$  the pixel is a parabolic point

DET and Gaussian Curvature have the same sign because the denominator of equation 3 is always positive. This means near a corner, DET gives an elliptic and hyperbolic part (respectively a positive and negative response) on both side of the edge. Moreover at these locations, DET has an elliptic maximum (positive maximum in the all directions) but does not have an hyperbolic maximum (negative minimum in the all directions). DET have a hyperbolic maximum only in particular direction (see section 3) but, this elliptic point detection doesn't allow to locate the corner accurately as it will be shown in section 3.

However, we can remark an interesting characteristic : the location of elliptic maximum point is *always inside the corner*, independently of the local image contrast. This property will be illustrated in section 3 and will be used for our approach.

Dreschler and Nagel [Dre82] proposed an operator based on Gaussian Curvature principle. Basically, this operator consists of the following rules :

1. Determine Gaussian curvature
2. Select locations of extremal Gaussian curvature
3. Match for each maximum positive Gaussian curvature such as E (ie elliptic point) with a location of maximum hyperbolic point such as H. Moreover, the directions of those principal curvatures at E and H have opposite sign and are approximately aligned.
4. Select the point T where this principal curvature crosses zero. This corresponds to the point of maximum slope on the curve between E and H over the gray-level surface image.

Three remarks can be made about this operator:

- The point T has its principal curvature equal to zero. This involves  $\kappa_{min} \kappa_{max} = 0$ . Therefore, the point T that this operator will detect will be a parabolic point.

- A theorem of differential geometry [Lip69] says :  
Let  $\gamma$  a regular curve on a surface  $\Omega$  with an inflection point  $M$  (second derivative in  $\gamma$  direction is zero), then  $M$  is a parabolic point or an hyperbolic point.  
In our problem,  $M$  is the corner and this theorem involves that  $M$  isn't necessarily a parabolic point. So, the corner is not necessarily detected by the Dreschler-Nagel's operator.
- The last remark is about maximum hyperbolic point location. We will show in the next section that
  1. The Gaussian curvature doesn't always get a maximum hyperbolic point in all directions. It depends on the corner angle. But a maximum hyperbolic exists always in special directions as bissector direction
  2. the location of maximum hyperbolic depends on the corner angle (cornerness) and for high cornerness level, this location is inside the corner ! Guiducci has already shown this characteristic (see [Gui88] Figs 3 and 4).

Kitchen and Rosenfeld [Kit82] proposed a measure of cornerness based on the change of gradient direction along an edge contour multiplied by the local gradient magnitude. They derived the following expression for cornerness :

$$K = \frac{I_{xx}I_y^2 + I_{yy}I_x^2 - 2I_{xy}I_xI_y}{I_x^2 + I_y^2} \quad (4)$$

Kitchen and Rosenfeld found that the local maximum of this measure isolated corners especially with a non maximum suppression process applied on the gradient magnitude before its multiplication with the curvature. In fact , it can be shown ( see for example Torre and Poggio [Tor86]) that  $K$  is the explicit representation for the second directional derivative in the direction orthogonal to the gradient.

Nagel [Nag83a] showed that the Dreschel-Nagel's approach and the Kitchen-Rosenfeld's approach are equivalent if the heuristic of non-maximum suppression along the gradient is applied to the gradient before multiplying by the gradient magnitude.

Zuniga and Haralick [Zun83] proposed an operator with a facet model approach. They assume that the grey level image  $f(x,y)$  can be modeled by the following bi-cubic polynomial surface :

$$I(x,y) = k_1 + k_2x + k_3y + k_4x^2 + k_5xy + k_6y^2 + k_7x^3 + k_8x^2y + k_9xy^2 + k_{10}y^3 \quad (5)$$

Computing the cornerness as the rate of change in gradient angle yields the following measure :



$$\kappa = -2 \frac{(k_2^2 k_6 - k_2 k_3 k_5 + k_3^2 k_4)}{((k_2^2 + k_3^2)^{\frac{3}{2}})} \quad (6)$$

If a point is an edge and this measure is above a given threshold, then the point is declared as a corner.

Shah and Jain [Sha84] showed that the only difference between the two expressions (4) and (6) is the factor  $\sqrt{(I_x^2 + I_y^2)}$  which is the gradient magnitude.

Recently, Noble [Nob88] tried to give a theoretical formulation for the corner detection problem using differential geometry. She outlined the principles underlying the Plessey corner detector [Har87] which is based only on first differentials :

$$C_p = \frac{\text{Trace}(\hat{C})}{\text{Det}(\hat{C})} \quad (7)$$

where  $\hat{C}$  is the following matrix :

$$\hat{C} = \begin{bmatrix} \hat{I}_x^2 & I_x \hat{I}_y \\ I_x \hat{I}_y & \hat{I}_y^2 \end{bmatrix} \quad (8)$$

and where  $\hat{I}$  denotes the smoothing operation on  $I$ .

In the case where the first derivatives at each pixel can be approximated by a first order Taylor's expression and for a Gaussian smoothing operator, it can be shown that this measure can be expressed as the sum of two components :

$$\hat{C} = \begin{bmatrix} I_x^2 & I_x I_y \\ I_x I_y & I_y^2 \end{bmatrix} + \sigma^2 \begin{bmatrix} I_{xx} & I_{xy} \\ I_{xy} & I_{yy} \end{bmatrix}^2 \quad (9)$$

It has to be pointed out that this is exactly the  $C$  matrix introduced and used by Nagel [Nag83b] in order to detect corners. As noted by Noble, this detector is only suitable for L-junctions, and its performance is unpredictable on higher-order structures. In fact, we will show in the last part of this paper that this measure suffers also from the delocalization problem that affects all the previous approaches.

Harris and Stephen [Har88] considered a slightly modified version of the Plessey corner detector. From Moravec's work [Mor77] and Barnard and Thompson's work [Bar80], they define a measure based on the following operator:

$$R(x, y) = \text{Det}[\hat{C}] - k \text{Trace}^2[\hat{C}] \quad (10)$$

This means that  $R(x, y)$  can be interpreted as the difference between Gaussian curvature and weighted function of square average curvature i.e if  $\kappa_{min}$  et  $\kappa_{max}$  are the principle curvature of the surface at the point  $(x, y)$ ,

$$R(x, y) = \kappa_{min}\kappa_{max} - k(\kappa_{min} + \kappa_{max})^2 \quad (11)$$

Harris gives a value of  $k$  equal to 0.04 for providing discrimination against high contrast pixel step edges. After that, the operator output is thresholded for the corner detection. Harris tried to find an invariant measure for stereoscopic problem, but doesn't give any details about the corner localization precision. In fact on running this algorithm on synthetics data, it is easy to find that the detected corners are not well localized.

Guiducci [Gui88] tried to give a formal representation of corner points in an image based on the differential geometry. He used three characteristics which are the amplitude  $A$  of the wedge, its aperture angle  $\theta$  and a parameter  $\sigma$  that is a measure of the smoothness of the wedge. This work is very interesting because in the sense that it shows localization variations of the extrema and zero of Gaussian curvature. In particular, Guiducci showed that for a  $\theta \in [\pi, \pi/2]$ , the hyperbolic extrema is always outside the corner, and for  $\theta < \pi/2$ , the hyperbolic and elliptic extrema are inside the corner. For  $\theta = \pi/2$ , the location of hyperbolic extrema is exactly the localization of corner.

We refer the reader interested by other kinds of approaches to the following references [Hua86], [Ran89] and [Kru89].

### 3 An analytical study

In this section, we consider a corner model and study its behaviour in the scale space. This allows us to derive results that clarify completely the behaviour of some well known approaches used in the problem of corner extraction. In particular, we have found that some of them are inadequate for an exact localization of the corner. Based on this study, we will present an approach that allows us to correct this drawback and to get the exact position. This approach makes use of two important properties of the corner in the scale space : First, the well known property that the Laplacian image is zero at the exact position of the corner, and second a property associated to the measure we propose to use in order to get the corner. It will be shown that corners extracted using this measure move in the scale space on a line passing through the exact position of the corner. We then combine these properties in order to get the exact position of the corner.

### 3.1 Notations and definitions

We introduce here some functions that will be largely used in the rest of the paper.

Let  $g(x)$  denote the zero-mean Gaussian filter :

$$g(x) = \frac{1}{\sqrt{2\pi}} e^{-\frac{x^2}{2}} \quad (12)$$

The two-dimensional Gaussian filter  $G$  can be expressed as :

$$G(x, y) = g(x)g(y) \quad (13)$$

Following Berzins [Ber84], we work in coordinate system where the unit length is equal to the scale factor  $\sigma$  of the filter. In order to convert the results into a more general coordinate system  $(X, Y)$ , we use the following transformation:

$$\begin{cases} x = \frac{X}{\sigma} \\ y = \frac{Y}{\sigma} \end{cases} \quad (14)$$

Let  $\Phi$  denote the error function given by :

$$\Phi(x) = \int_{t=-\infty}^x g(t)dt \quad (15)$$

Let  $U$  define the unit step function

$$U(x) = \begin{cases} 1 & \text{if } x > 0 \\ 0 & \text{otherwise} \end{cases} \quad (16)$$

The response of the 2D Gaussian filter  $G$  for a 2D input function  $I$  can be computed by evaluating the following convolution integral

$$S(x, y) = \int_{\alpha=-\infty}^{+\infty} \int_{\beta=-\infty}^{+\infty} G(\alpha, \beta) I(x - \alpha, y - \beta) d\alpha d\beta \quad (17)$$

### 3.2 A Corner Model

An ideal corner with one edge along the  $x$  axis and an angle  $\theta$  can be modeled by the following 2D step function.

$$I_\theta(x, y) = U(x)U(mx - y) \quad (18)$$

where  $m = \tan(\theta)$ .

If we convolve this 2D step function with the 2D Gaussian filter given by 13, we get the following filtered image  $S(x, y)$ :

$$S(x, y) = \Phi(x)\Phi(y) - \int_{\alpha=-\infty}^x g(\alpha)\Phi(y - mx + m\alpha)d\alpha \quad (19)$$

This equation describes a Gaussian filtered corner with angle  $\theta$  localized in the origin point  $(0, 0)$ . Figure 1 illustrates such a surface for the case of a right angle model.

Let us make the following changes of variables:

$$\begin{aligned} u &= x\sin(\theta) - y\cos(\theta) \\ v &= x\cos(\theta) + y\sin(\theta) \end{aligned} \quad (20)$$

The components  $S_x(x, y)$  and  $S_y(x, y)$  of the gradient vector  $\vec{\nabla}S(x, y)$  are then given to be

$$\vec{\nabla}S(x, y) = \begin{bmatrix} g(u)\Phi(v)\sin(\theta) \\ g(y)\Phi(x) - g(u)\Phi(v)\cos(\theta) \end{bmatrix} \quad (21)$$

The norm of the gradient vector can be easily calculated. Figure 2 illustrates the surface  $\|\vec{\nabla}S(x, y)\|$  for the case of a right angle model. It is worth noting how the gradient magnitude looks like near the exact position of the corner (i.e the point  $(0, 0)$ ). The magnitude decreases near the origin point and affects the edge extraction process as it will be shown in the next subsection.

As it can be seen in the appendix, the Hessian matrix is important for the description of surfaces. The elements of such a matrix can be calculated by deriving two times in the  $x$  and  $y$  directions, the surface  $S(x, y)$ . Applying this to our corner model surface yields the following elements :

$$\begin{aligned} S_{xx}(x, y) &= g(u)\sin(\theta)(g(v)\cos(\theta) - u\Phi(v)\sin(\theta)) \\ S_{xy}(x, y) &= S_{yx}(x, y) = g(u)\sin(\theta)(u\Phi(v)\cos(\theta) + g(v)\sin(\theta)) \\ S_{yy}(x, y) &= -yg(y)\Phi(x) - g(u)\cos(\theta)(u\Phi(v)\cos(\theta) + g(v)\sin(\theta)) \end{aligned} \quad (22)$$

All the results derived here will be used in the next subsections

### 3.3 About the way to extract edges

It is well known that edges can be extracted from an image using the non maximum suppression scheme [Can86] ,[Der87] or the zero-crossing scheme [Ber84]. In this subsection, we briefly remind the main difference between both approaches in the case where corners have to be detected [Ber84] ,[Berg87]. In the first approach, edges are extracted as local maxima of the gradient magnitude in the gradient direction. This is equivalent to extract points where the second directional derivative of the gradient magnitude image along the gradient direction is equal to zero. An explicit representation of the second directional derivative in the gradient direction  $\mathbf{n}$  can be found to be :

$$\frac{\partial^2 S}{\partial \mathbf{n}^2} = \frac{S_{xx}S_x^2 + 2S_xS_yS_{xy} + S_{yy}S_y^2}{(S_x^2 + S_y^2)} \quad (23)$$

The location of the zero-crossings of ( 23) corresponds to the location of the discontinuity in the 2D step filtered function 19 extracted following the non-maximum suppression scheme. Figure 3 illustrates the curve that represents the set of points extracted through the use of this measure in the case of a right angle. This figure illustrates the well-known rounding effect of the edge extraction with the non-maxima suppression scheme [Berg87]. In order to better appreciate the displacement of the extracted edges, let's take the particular edge point that belongs to the line bissector and look for its displacement from the its correct position (i.e the origin point (0,0) ), we have found the following results. For a right angle the displacement found was equal to  $.7151\sigma$  while it was found to be  $1.329\sigma$  and  $1.893\sigma$  for angles with  $\pi/4$  and  $\pi/8$  respectively. The sharper the angle is, the bigger will be the displacement.

In the second approach, edges are extracted as zero-crossings in the Laplacian image given by :

$$\nabla^2 S(x, y) = S_{xx}(x, y) + S_{yy}(x, y) \quad (24)$$

Dealing with the corner described by (19) leads to the following expression for the Laplacian :

$$\nabla^2 S(x, y) = -(yg(y)\Phi(x) + ug(u)\Phi(v)) \quad (25)$$

Equation (25) can be solved numerically to find the contours where the Laplacian equal to zero. The resulting contours are shown in Figure 4 for the Gaussian filtered

right angle. Let us remind that both  $x$  and  $y$  are given in units of standard deviations  $\sigma$ . This illustrates very well the rounding effect due to the use of the Laplacian instead of the non-maxima suppression scheme. Following [Ber84], the largest deviation of the computed edge from the true edge can be found to be for  $x = .839\sigma, y = -0.295\sigma$ .

From these remarks, an important point to note is that the Laplacian allows to recover exactly the position of the corner since it is equal to zero at the origin. This is not the case for the non-maximum suppression scheme where the point presenting the highest curvature is far away of  $.506\sigma$  from the exact position of the corner (i.e the origin point  $(0, 0)$ ). We will make use of this important point in order to correct the position of the extracted corner.

In order to better appreciate the difference between the Laplacian and the non-maximum approach, we can interpret the Laplacian as the sum of the second directional derivatives in any two orthogonal directions. Therefore, noting by  $\mathbf{n}$  the gradient direction and by  $\mathbf{n}_\perp$  the contour direction, the Laplacian can also be expressed as follows:

$$\nabla^2 S(x, y) = \frac{\partial^2 S}{\partial \mathbf{n}^2} + \frac{\partial^2 S}{\partial \mathbf{n}_\perp^2} \quad (26)$$

It is easy to see that the first term is exactly the term used in order to detect edges following the non-maximum suppression scheme. In another hand the second term that differentiates between both approaches has a simple interpretation in terms of the normal curvature. Up to a gradient norm factor, it is the Kitchen and Rosenfeld's measure used to detect corner.

All these points have interest in that they answer the question of what is the reason of the different comportment of the Laplacian and the non-maxima scheme and that they will be used in the analysis of some classical corner extraction schemes and in the way to correct the corners localization.

### 3.4 Analysis of Some classical approaches for Corner Extraction

In this subsection, we will discuss and analyze the comportment of three classical measures that have been proposed and used in the corner detection, namely Beaudet, Nagel and Rosenfeld's approach's.

Following Kitchen and Rosenfeld [Kit82], the corner points can be detected using the measure given by equation 4. As noted previously, this measure is the explicit representation for the second directional derivative in the direction orthogonal to the gradient and corresponds at the curvature scaled by the gradient magnitude. Kitchen and Rosenfeld found that the local maximum of this operator isolated corners especially with a non maxima suppression process applied on the gradient magnitude.

In the previous section, we have shown that the edges extracted using the non-maxima scheme are not well localized near a corner due to the rounding effect. This effect is well illustrated in figure 3. This means in particular that the corners extracted with Kitchen and Rosenfeld's approach will belong to the curve shown in figure 3 and thus will not be well located. However it is worth noting that this measure allows to recover exactly the corner position if it is used without to be combined with the gradient magnitude. This is well illustrated by Figure 5. It represents the measure of Rosenfeld scaled by  $(-1)$  on the line  $y = -x$  (i.e along the edge direction or the normal direction of the gradient for a right angle). Therefore, a local extrema exists at the origin point. Dealing with the same measure for sharper angles, it can be shown that this extrema does not displace on the scale-space. This stability in the scale space has to be considered because all real images are smoothed in order to remove noise. Therefore it is important to know if this smoothing process has any influence on the measure we use or not. A possible improvement of this approach is to use the edges extracted as zero-crossings and not as local maxima, since it has been shown in the previous section that in the exact corner points  $(0,0)$ , the Laplacian image is equal to zero. However, a big drawback remains for this measure: the fact that it uses the edge direction. We have to know exactly this information. In real images, this information is obtained from the directional derivatives in the  $x$  and  $y$  directions. These informations are not reliable, in particular near the points we would like to detect: the corners. It is natural then to try to avoid using such informations using measure much more stable than the gradient or edge direction and that presents a global extrema (i.e extrema in all the directions). Beaudet's and Nagel's approach use such measure but we will show how their approach suffer from another problem not considered in their analysis : the localization problem.

As described in the first section of this paper, Beaudet's approach is based on the use of the determinant of the Hessian matrix associated to the intensity image and called *DET*. Figure 6 illustrates the surface describing Beaudet's measure. We remark that we have an important local maximum in *all the directions* indicating that this approach is much more stable than the one proposed by Kitchen and Rosenfeld. Using a steepest descent based algorithm starting from the point  $(x = 1, y = 1)$ , we found that the local maximum in all the directions for such surface is located exactly in the bissector line at  $(x = 1.17134\sigma, y = 1.17134\sigma)$  for a right angle. Therefore, detecting the corner point as the point where this local maximum occurs leads to a displacement between the true point and the one detected equal to  $1.6565\sigma$ . Dealing with an angle of  $\frac{\pi}{4}$  leads to displace the position of the local maximum to  $(x = 2.58231\sigma, y = 1.06963\sigma)$  ( i.e in the bissector line of the angle ). The displacement from the true corner point is in this case equal to  $2.795\sigma$ . For sharper angle, the local maximum is pushed away on the bissector line. Figures 7 and 8 illustrates this displacement effect. They represent the *DET* measure on the bissector lines for angles equal to  $\pi/2$  and  $\pi/4$  respectively. It is clear that the local maximum does not

locate correctly the corner point. What appears from these figures is that the local extrema of measure proposed by Beaudet are not stable in the scale-space. Since the displacement is function of the standard deviation  $\sigma$  used in the filtering proces, this measure does not allow to locate exactly the corner. However, since a local maximum in all direction is rather much more easier to extract that maximum along a specific direction ( because of the accuracy on that direction ), we will show in the next subsection how we can use this measure in order to extract correctly corners.

The third approach we want to analyze is the one proposed by Dreshler and Nagel [Dre82],[Nag83a]. It is based on the Gaussian curvature. We first detect positive as well negative extrema of the Gaussian curvature. It is worthnoting that since the corner is located at a zero-crossing of one of the main curvature, it corresponds also to a zero-crossing of the Gaussian curvature. Using a steepest descent based algorithm starting from the point  $(x = 1, y = 1)$ , we found that the local maximum in all the directions for the Gaussian curvature is located exactly in the bissector line at  $(x = 1.216\sigma, y = 1.216\sigma)$  for a right angle. Dealing with an angle of  $\frac{\pi}{4}$  leads to displace the position of the local maximum to  $(x = 2.634\sigma, y = 1.09\sigma)$  ( i.e in the bissector line of the angle ). However using the same technique we have not been able to find the local minima in all the directions. This is because a minima in all the directions does not exist. Figure 9 illustrates the Gaussian curvature for a right angle. What appears from this figure (and from many others but not included here ) is that the positive extrema is very well detected but there are no negative extrema in all directions. This means that it will be difficult to extract this minima. However this minima exists in the edge direction or bissector line direction as shown by Figures 10 and 11. From these figures, it appears that the zero crossings of one of the main curvature ( and consequently a zero-crossing of the Gaussian curvature ) does not give the correct position of the corner. Another important point to note is that the extrema locations of the Gaussian curvature as well as the zero crossing of the Gaussian curvature on the bissector line moves in the scale space. This leads to the fact that the corner extracted following this approach are not well located. In fact, this approach suffers from the same problem than Beaudet's approach. We will show in the next subsection how we can make use of these importants points in order to better locate the extracted corners.

The last approach that have been tested is the one proposed by Noble and known as the Plessey corner detector and its slightly improved version as proposed by Harris and described in the first section of this paper. Using an angle of  $\Pi/2$  and a  $k$  value of 0.04 as proposed by Harris, we have been able to find that the position of the local maximum in all the direction is located at  $x_{max} = y_{max} = .7611\sigma$  and thus does not corresponds to the exact position of the corner ( $\sigma = 1$  was used for the Gaussian smoothing operator).



### 3.5 Combining informations to extract accurate corners

Following the analysis that have been done, two important points have to be noted :

- The exact position of a corner can be detected as a stable zero-crossing in the scale-space.
- The local maxima in Beaudet and Nagel's measures moves in the scale space along the bissector line that passes through the exact position of the corner point.

We have combined these two observations in order to extract corner as follows : First a Laplacian image is calculated. Second, Beaudet's measure at two scales are calculated and an extrema detection in all directions is performed. Around each detected extrema in the image corresponding to the first scale, we look in the second image for the position of the local maxima. Once this second maxima detected, we look for the exact position of the corner as the point that belongs to the line segments joining the two positions and where a zero-crossing occurs in the Laplacian image.

With such approach, we have combined the two important points that we have mentioned. Experimentally, this approach has been found to be reasonably stable. However some difficulties may arise. In particular for angle less than  $\pi/4$ , the displacement is very important, and thus we have to look in a bigger neighborhood than the one implemented in order to have the expected results.

## 4 Some Experimental results

In this section, we give the first experimental results obtained on running the new approach described in the previous section on 512.512 image with 256 grey level. The goal is to identify corners present in this image at pixel precision. All the low-level process required in the approach ( smoothing and deriving steps) is done using the Gaussian filter operator and its derivatives.

For the corner detection, the algorithm implementation basically consists of the following steps:

- Using equation 1, compute two images  $DET_1$  and  $DET_2$  corresponding at two different values  $\sigma_1 < \sigma_2$  for the scale space. In our implementation, we have taken  $\sigma_1 = 1$  and  $\sigma_2 = 2$ .
- Detect and threshold all the local maxima (only positive value) of  $DET_1$  and  $DET_2$ . A threshold equal to 200 has been used for both  $DET_1$  and  $DET_2$ .

- For each position  $(x_2, y_2)$  of a local maxima in  $DET_2$ , search for a local maxima in  $DET_1$ . This searching process is implemented in spiral centered on  $(x_2, y_2)$ , limited to a  $7 \times 7$  window and we take the first local maxima  $(x_1, y_1)$  which is found. In order to improve the precision in localization, for each detected local maxima we fit a quadratic surface around each local maxima  $(x_i, y_i)$  and select at a sub-pixel precision the corrected position of each local maxima.
- Compute the line equation joining  $(x_1, y_1)$  and  $(x_2, y_2)$ . This gives the estimate bissector line where the exact corner position must lie. Along this line, starting from  $(x_2, y_2)$  and moving in an opposite direction to  $(x_1, y_1)$ , validate the first zero-crossing location  $(X, Y)$  of the Laplacian as the exact localization of the corner at pixel resolution (if we get the minimum absolute value of laplacian pixel), or in sub-pixel resolution (if we track the exact zero-crossing by a curve fit on laplacian).

In order to test our approach on noisy synthetic data, we first considered the triangle shown in Figure 12. The corners extracted on such image are superimposed and indicated by the sign  $+$ . In order to test the robustness of the approach against noise, we have added a Gaussian noise with standard deviation  $\sigma$ , to this synthetic image with respectively a SNR of 14dB ( $\sigma = 10$ ) and 8.5 dB ( $\sigma = 20$ ).

The signal to noise ratio (SNR) is computed as follow :

$$SNR_{dB} = 10 \log \left( \frac{\sum \sum f(x, y)^2}{\sum \sum e(x, y)^2} \right) \quad (27)$$

where  $f(x, y)$  is the input image without noise and  $e(x, y)$  indicates the noise.

Figures 13 and 14 illustrate the results obtained for this example. The extracted corners are indicated by the sign  $+$  in the images. We have used  $\sigma = 2$  and  $\sigma = 1$  (resp.  $\sigma = 3$  and  $\sigma = 1$ ) for the noisy synthetic image with a SNR of 14db (resp. 8.5db) and we have computed the laplacian with  $\sigma = 2$ . The localization of the extracted corners is good except for the case 8.5dB where we have a 2 pixel shift on the sharper angle.

In order to illustrate some steps of the algorithm, Figures 15 to 17 and 18 to 19 show a local zoom of what happens near two corners of type  $\Pi/2$  and  $\Pi/4$  respectively. Detection of elliptic maximum and corner localization are shown using two different resolutions corresponding at  $\sigma_1 = 1$  and  $\sigma_2 = 2$ . The corrected position derived by the algorithm seems to be quite remarkable.

Figure 21 shows an example of the promising result we have obtained on running the algorithm on an entire real image. Almost all the corners have been well detected and corrected. Note that decreasing the threshold of maxima magnitude would have

resulted on more corners points detected on the image. The results obtained on running the algorithm on a triplet of trinocular stereo images are very stable and let us hope that the matching process will be much more easier and reliable using these features.

We are in the process of implementing the algorithm using a complete multi-scale representation using  $\sigma = 1$  to  $\sigma = 6$ . This will lead us to use a polygonal approximation of the line bissector instead of simply joining two points. Relating the width of the search window to the scale space used is also a point that we are considering.

## 5 Conclusion

A formal representation of corner detection has been shown in this paper. In particular, an analytical study that allows us to know exactly what is the behavior of some classical measures like the one proposed by Nagel, Beaudet or Kitchen has been developed. We have proposed a new approach in order to correct their faulty localization and shown the first experimental results on real data obtained that seems promising.

## 6 Acknowledgments

The authors would like to express all their acknowledgments to **Maple** and **Mathematica** for all the mathematical and graphical facilities.

## 7 Figures and Images

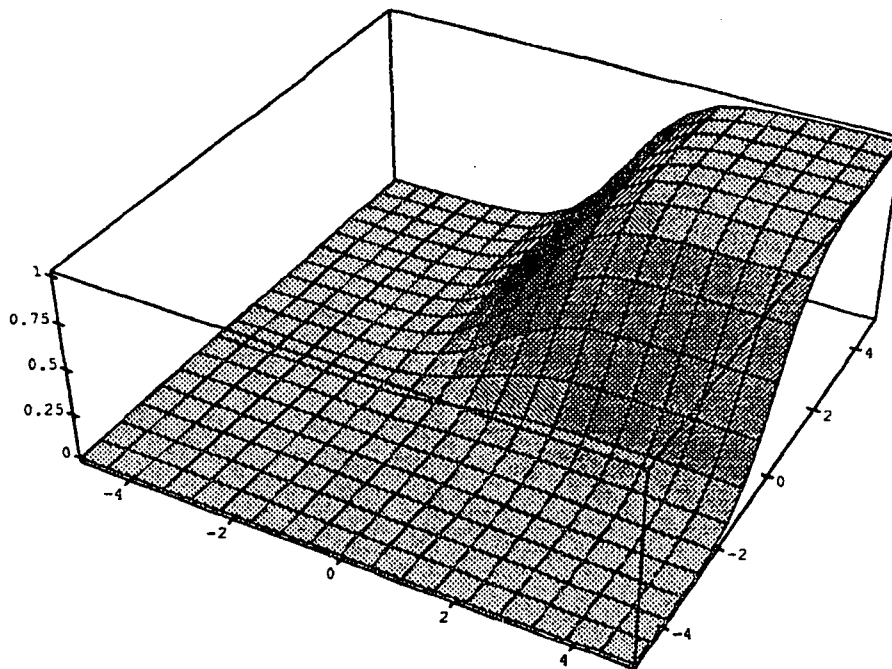


Figure 1: A Gaussian Filtered  $\pi/2$  Angle Model

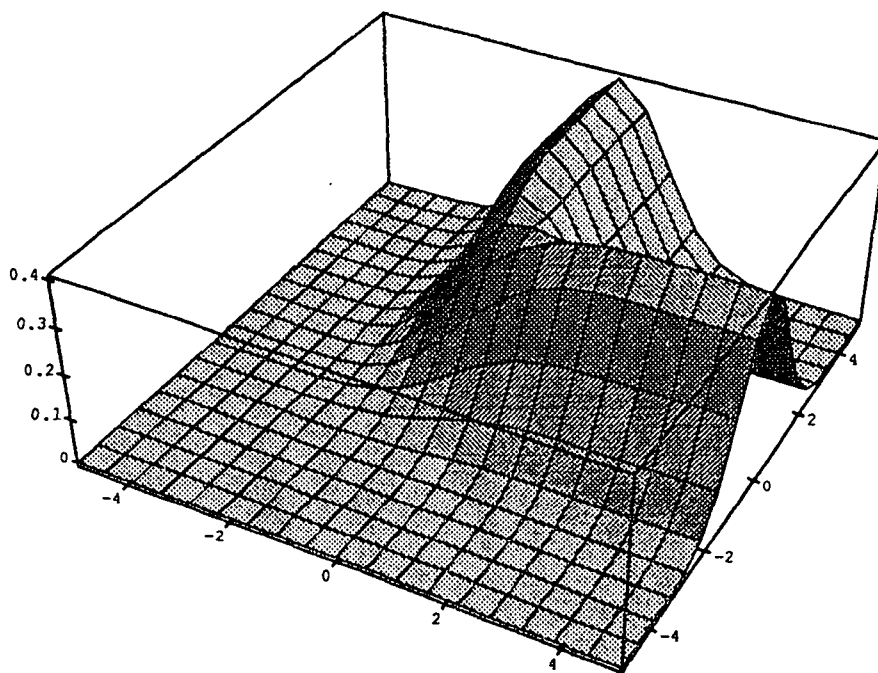


Figure 2: The Gradient Magnitude for a Gaussian Filtered  $\pi/2$  Angle Model

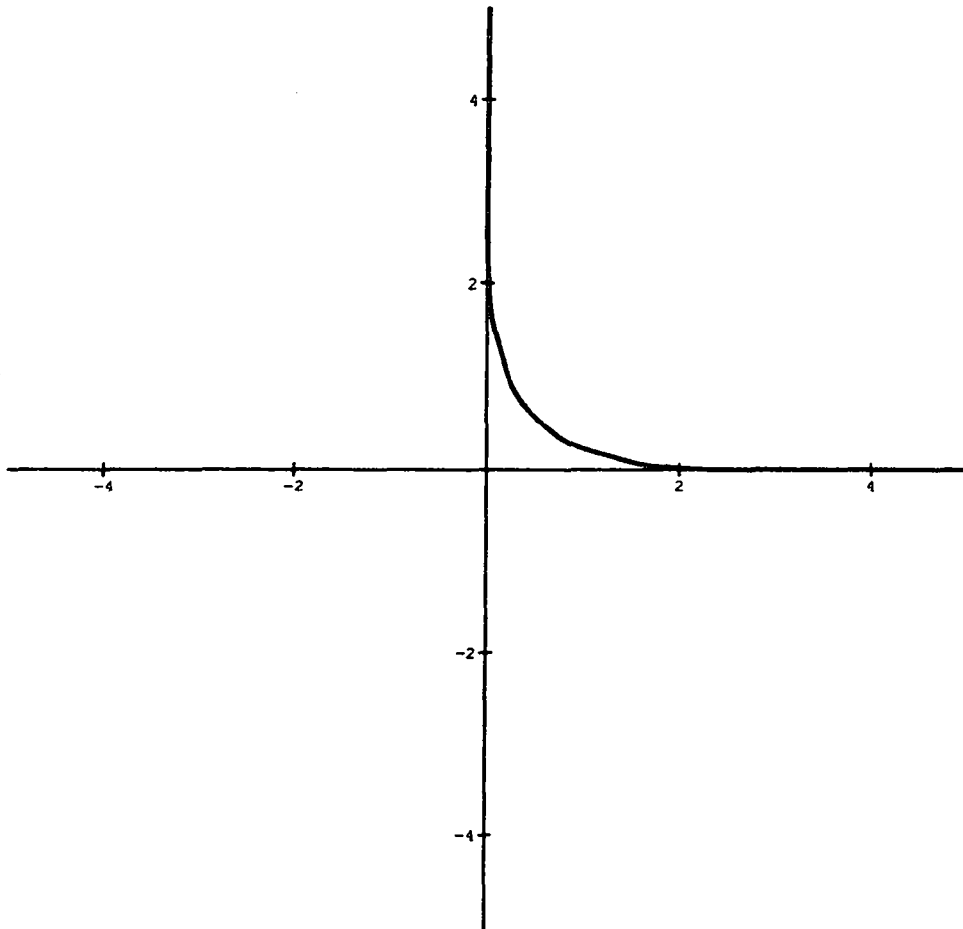


Figure 3: Edges Extracted as Local Maxima in the Gradient Direction for a  $\pi/2$  Angle Model

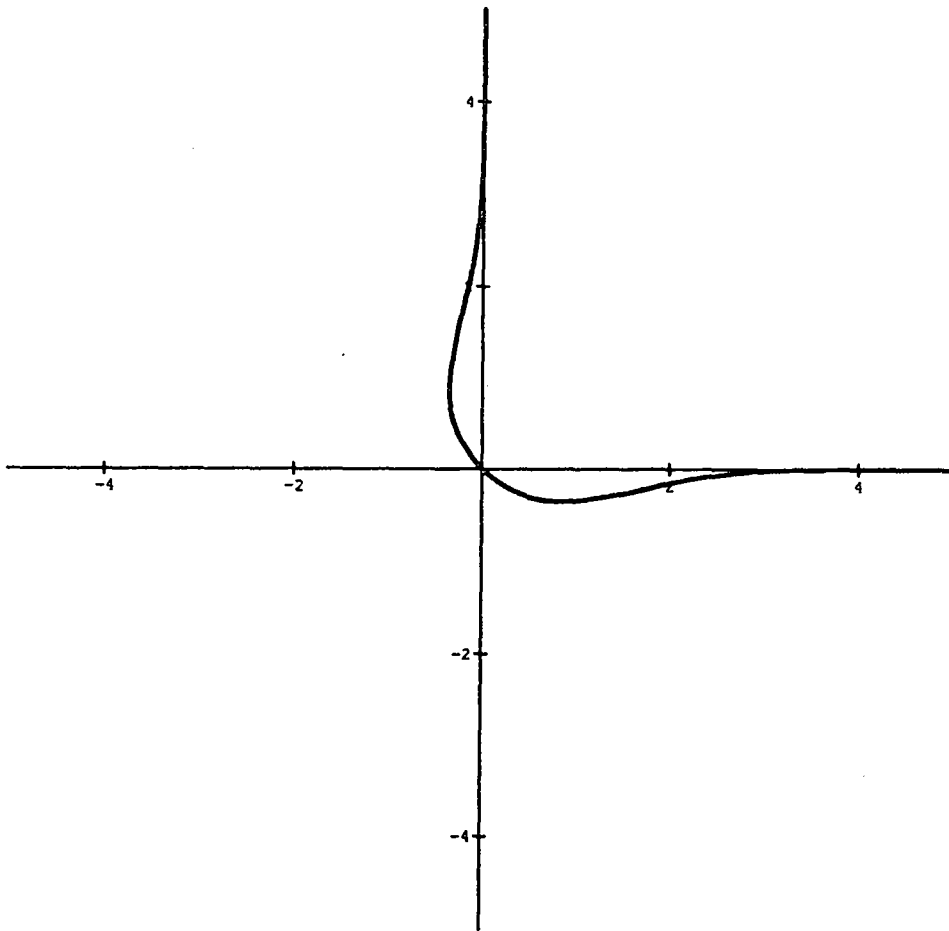


Figure 4: Edges Extracted as Zero-Crossings for a  $\pi/2$  Angle Model

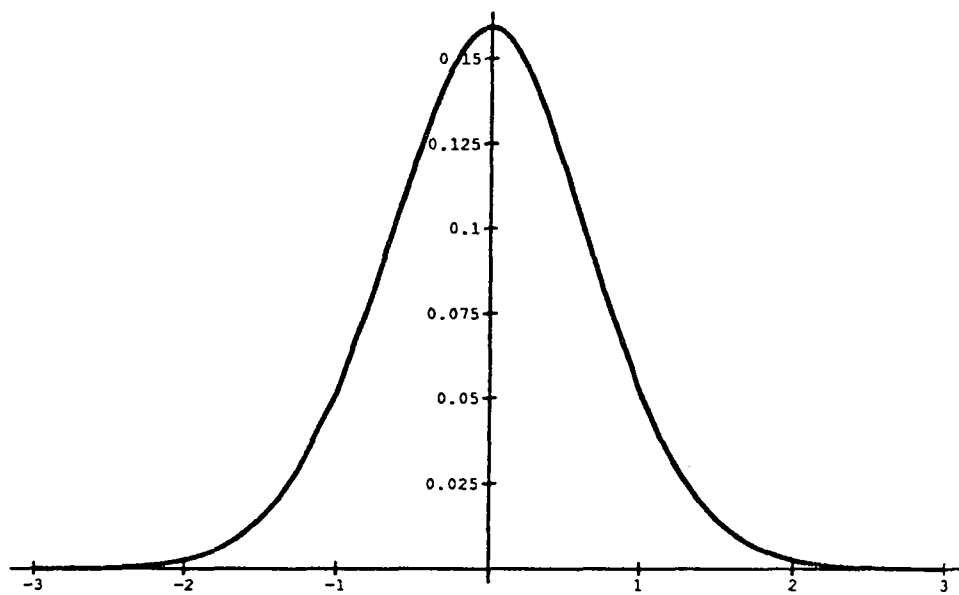


Figure 5: Rosenfeld's Measure Along the Edge Direction



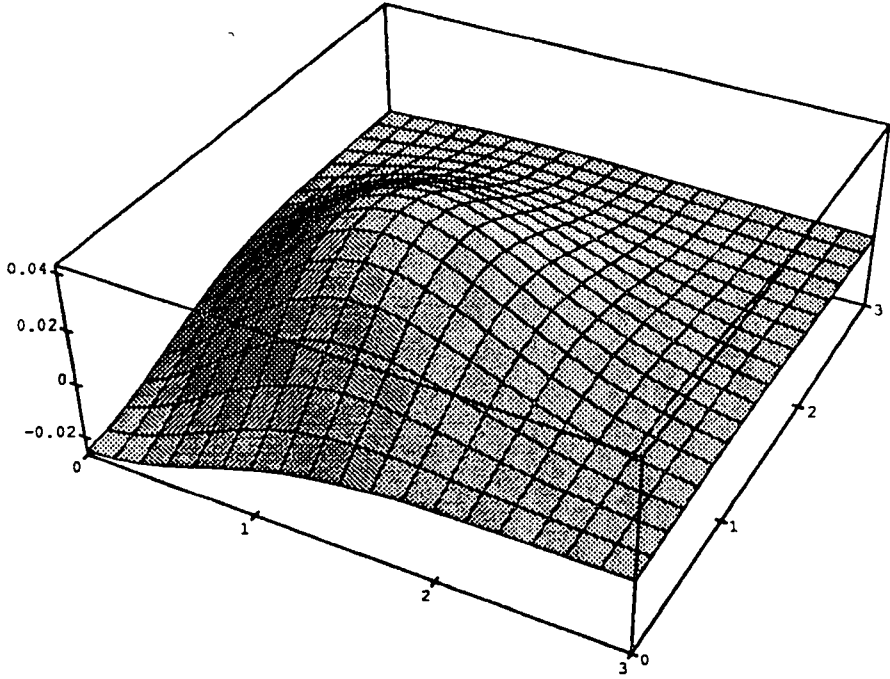


Figure 6: Beaudet's Measure

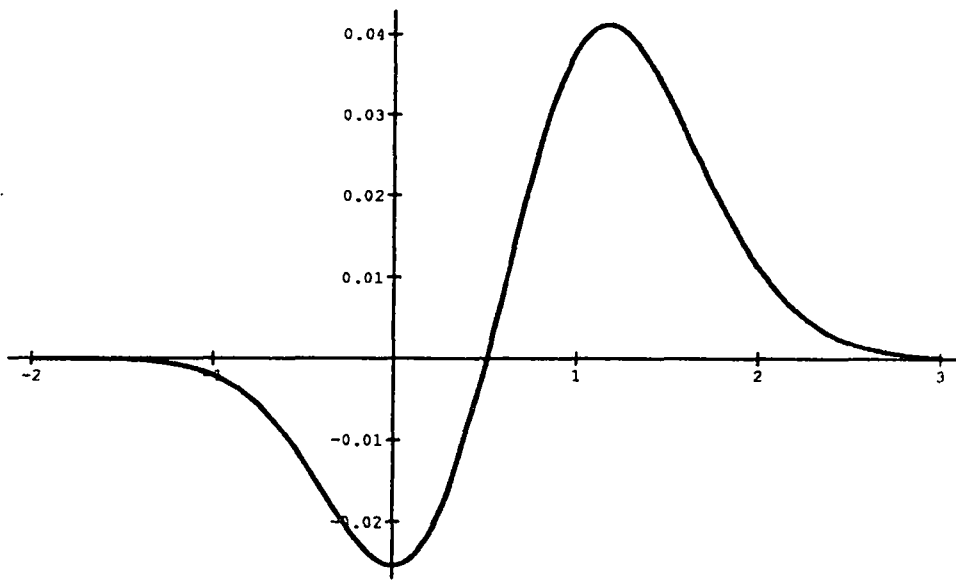


Figure 7: Beaudet's Measure on the Bisector line for a  $\pi/2$  Angle Model

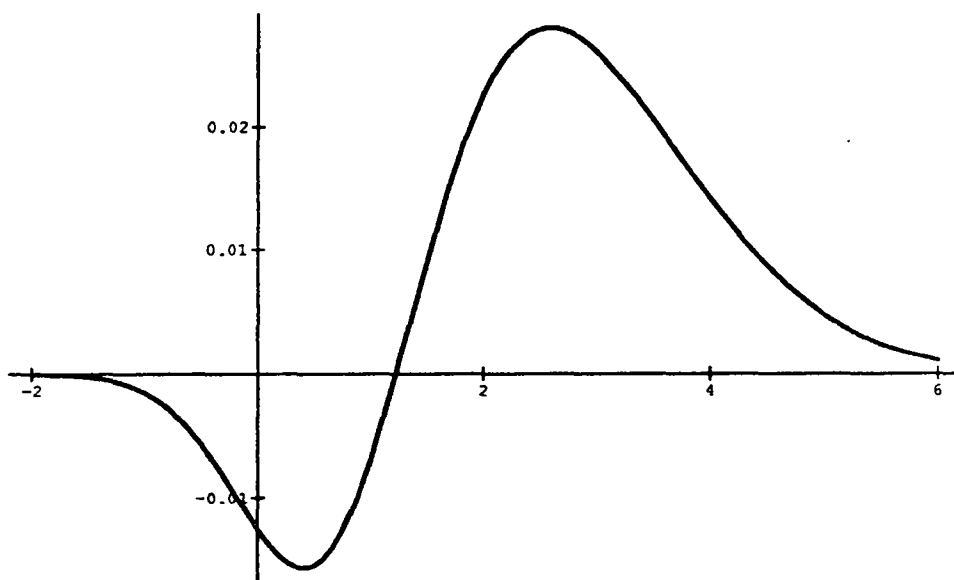


Figure 8: Beaudet's Measure on the Bisector line for  $a\pi/4$  Angle Model

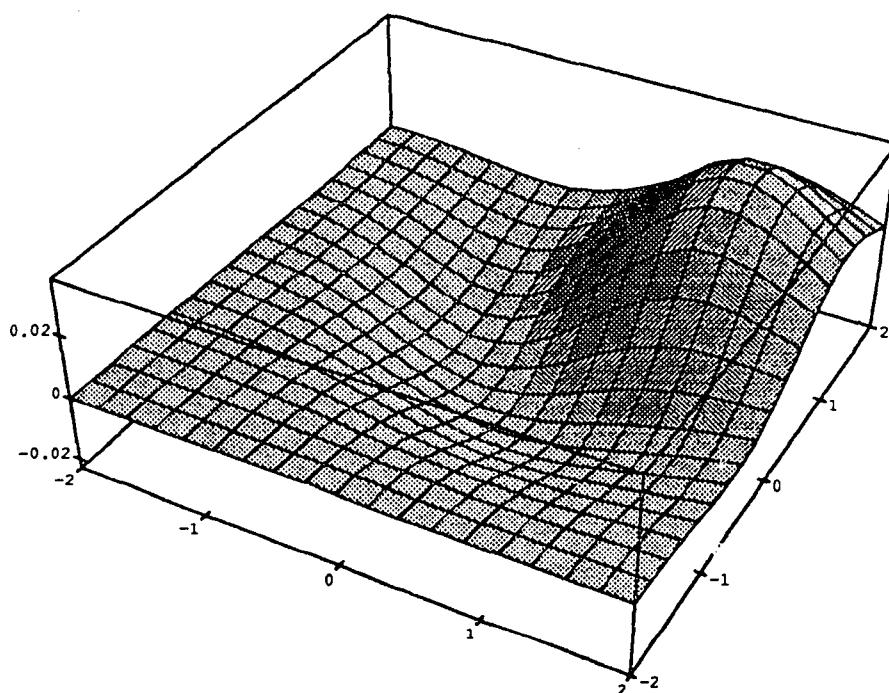


Figure 9: Gaussian Curvature for  $\pi/2$  Angle Model

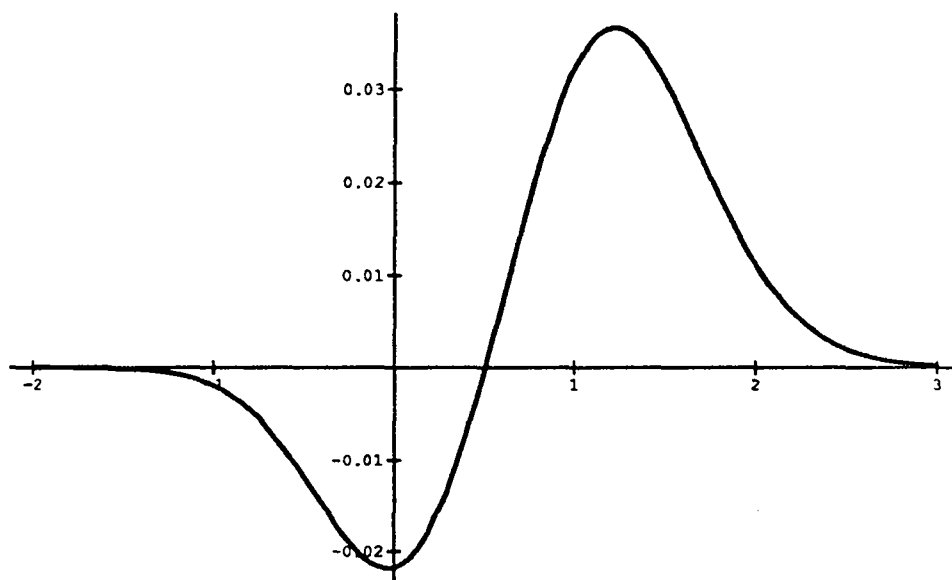


Figure 10: Gaussian Curvature on the Bisector line for  $\pi/2$  Angle Model

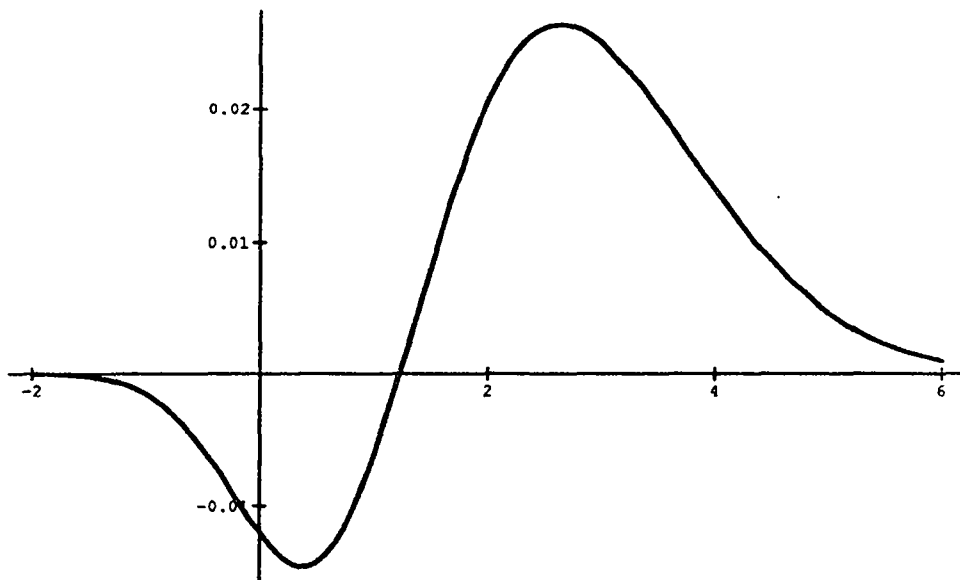


Figure 11: Gaussian Curvature on the Bisector line for  $\pi/4$  Angle Model

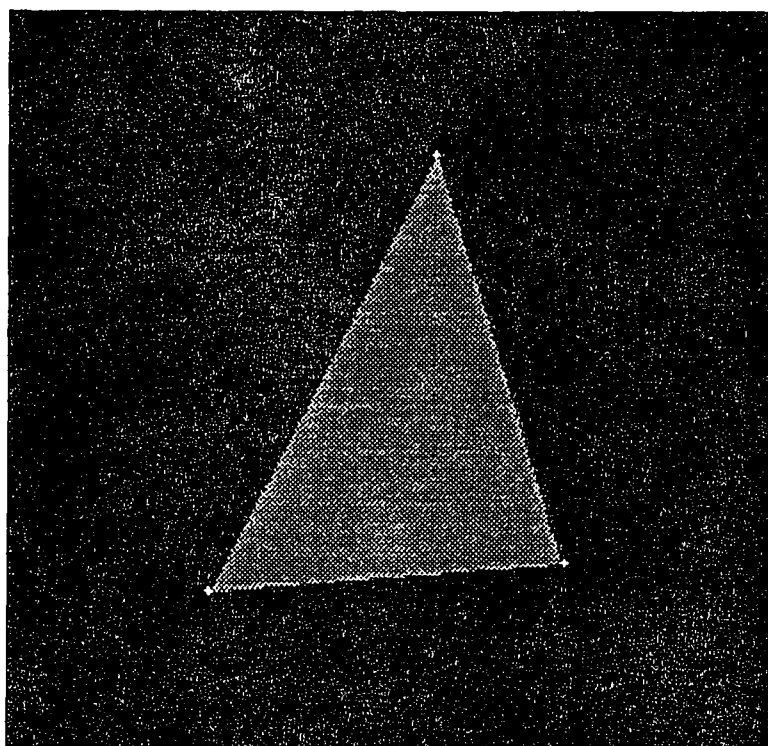


Figure 12: Corners extracted on a synthetic triangle

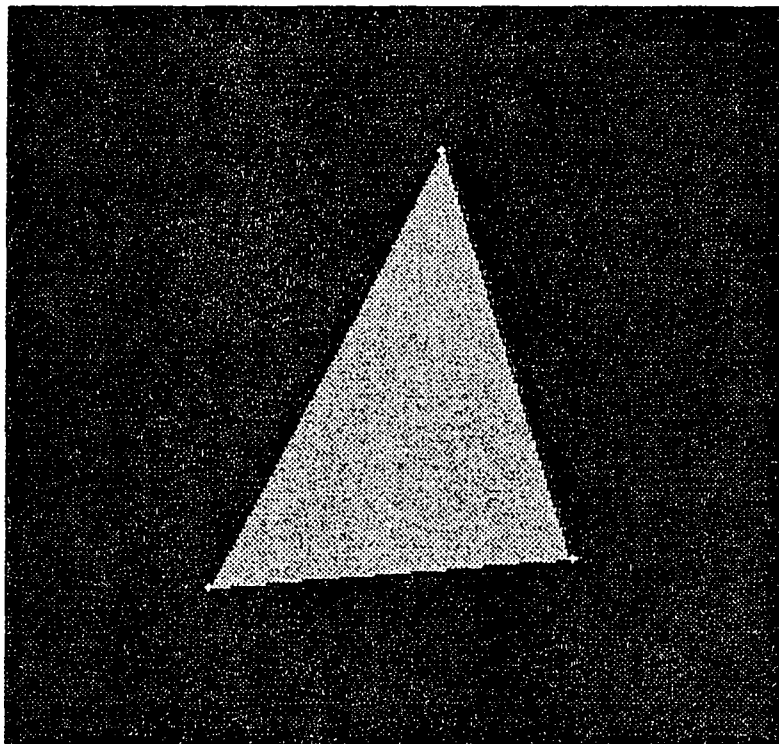


Figure 13: Corners extracted on a noisy synthetic triangle SNR=14db



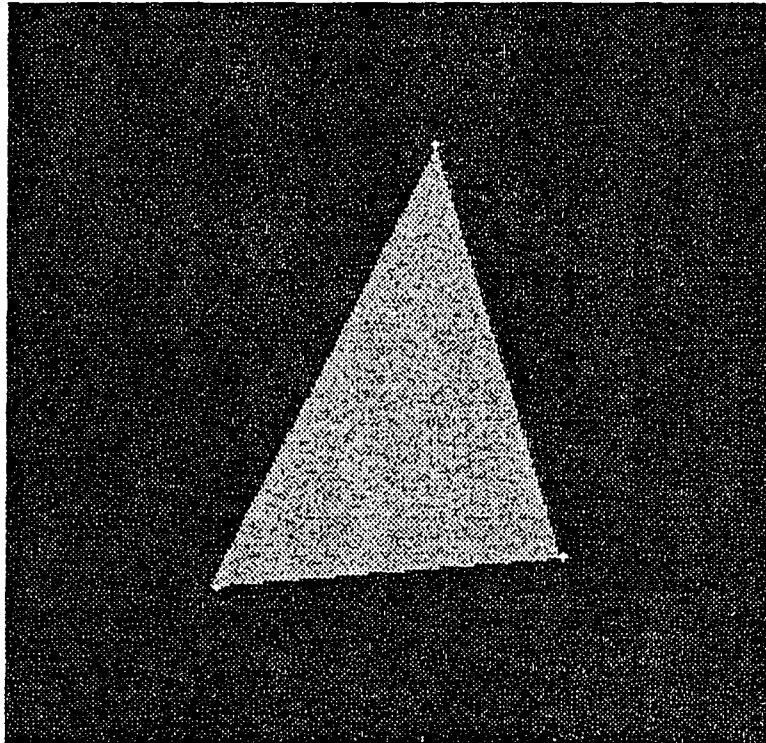


Figure 14: Corners extracted on a noisy synthetic triangle SNR=8.5db

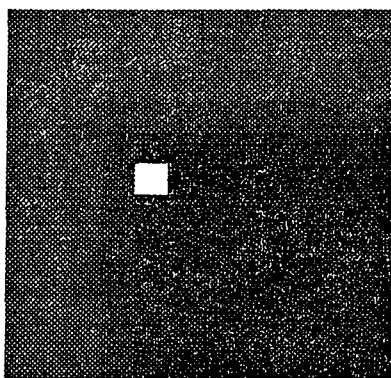


Figure 15:  $\pi/2$  type angle : Corner detected with  $\sigma=1$

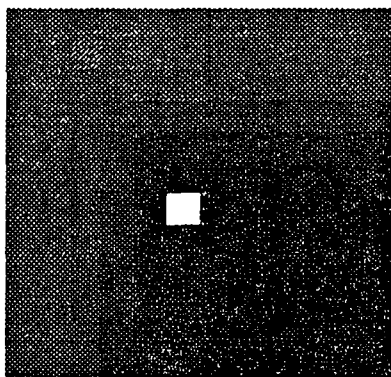


Figure 16:  $\pi/2$  type angle : Corner detected with  $\sigma=2$

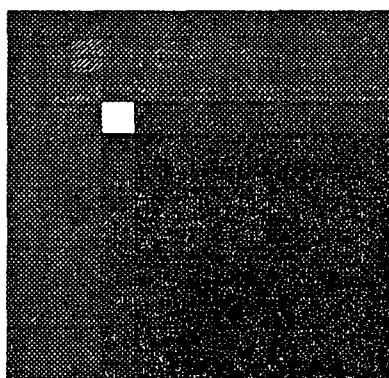


Figure 17:  $\pi/2$  type angle : Corrected position

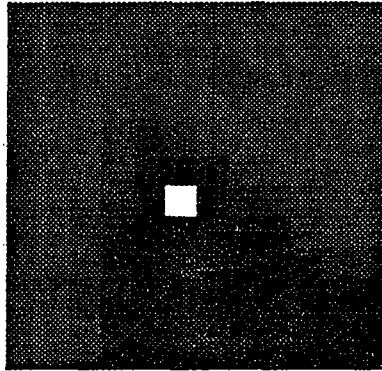


Figure 18:  $\pi/4$  type angle : Corner detected with  $\sigma=1$

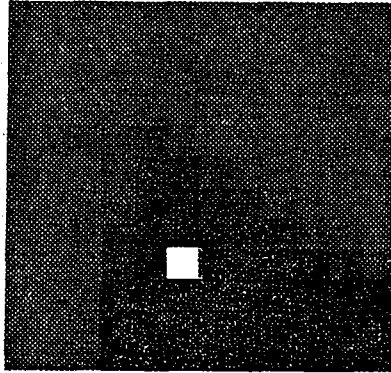


Figure 19:  $\pi/4$  type angle : Corner detected with  $\sigma=2$

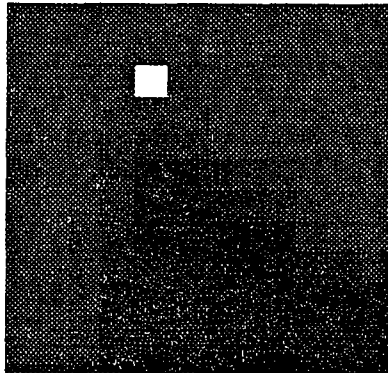


Figure 20:  $\pi/4$  type angle : Corrected position



Figure 21: Corners points detected on an indoor scene

$$\kappa = \frac{Ldx^2 + 2Mdx dy + Ndy^2}{Edx^2 + 2Fdx dy + Gdy^2} \quad (38)$$

At each point, a direction  $(dx, dy)$  is associated to the curvature  $\kappa$  given by the equation 38. There are two directions for which  $\kappa$  has maximum and minimum values. They are solution of the equations

$$\begin{aligned} \frac{\partial \kappa}{\partial(dx)} &= 0 \\ \frac{\partial \kappa}{\partial(dy)} &= 0 \end{aligned} \quad (39)$$

Using equation 38 and deriving yields the following equations:

$$\begin{aligned} (-L + \kappa E)dx + (-M + \kappa F)dy &= 0 \\ (-M + \kappa F)dx + (-N + \kappa G)dy &= 0 \end{aligned} \quad (40)$$

For a solution to exist,  $\kappa$  must satisfy

$$\kappa^2 - 2H\kappa + K = 0 \quad (41)$$

where the coefficients  $K$  and  $H$  denote the **Gaussian curvature** and the **mean curvature** respectively :

$$\begin{aligned} K &= \frac{LN - M^2}{EG - F^2} \\ H &= \frac{EN + GL - 2FM}{2(EG - F^2)} \end{aligned} \quad (42)$$

The solutions to equation 41 represent the maximum and minimum curvature at the given point and are called the **principal curvatures**

$$\begin{aligned} \kappa_{min} &= H - \sqrt{H^2 - K} \\ \kappa_{max} &= H + \sqrt{H^2 - K} \end{aligned} \quad (43)$$

Substituting  $\kappa_{min}$  and  $\kappa_{max}$  for  $\kappa$  in equation 41 yields the solutions  $(dx, dy)$  for the principal directions that are always orthogonal.

When  $H^2 = K$ ,  $\kappa_{min} = \kappa_{max}$  and the curvature is independent of direction. Such point is called an *umbilic* or *spherical* point since the surface locally approximates a sphere at that point.

The **Gaussian** and **Mean Curvatures** introduced above can easily be expressed as the product and average of the **Principal Curvatures**, respectively :

$$\begin{aligned}
K &= \kappa_{max}\kappa_{min} \\
H &= \frac{\kappa_{max}+\kappa_{min}}{2}
\end{aligned}
\tag{44}$$

It is worthnoting that if we define the matrix  $\beta$  as follows :

$$\beta = [\mathbf{G}^{-1}][\mathbf{H}] \tag{45}$$

It can be shown that  $K$  and  $H$  can easily be expressed as the determinant and half the trace of the matrix  $\beta$  respectively.

More details and results about the differential geometry of surfaces can be found in the reference [Lip69].

## References

- [Asa86] H. ASADA and M. BRADY: "The Curvature Primal Sketch" IEEE PAMI, Vol 8 1986, pp 2-14.
- [Bar80] S.T. BARNARD and W.B. THOMPSON : "Disparity analysis of images", IEEE PAMI, Vol2, No 4, July 1980, pp 333-340
- [Bea78] P.R. BEAUDET: "Rotational Invariant Image Operators", in Int, Conf Pattern Recognition 1978 pp 579-583.
- [Berg87] F. BERGHOLM : "Edge Focusing", IEEE PAMI Vol9, No 6 November 1987 pp 726-741
- [Ber84] V. BERZINS "Accuracy of Laplacian Edge Detectors", in CVGIP Vol27, 1984 pp 195-210
- [Can86] J.F. CANNY : "A Computational Approach to Edge Detection", IEEE PAMI Vol8, No 6 November 1986 pp 679-698
- [Der87] R.DERICHE : " Using Canny's Criteria to Derive a Recursively Implemented Optimal Edge Detector.", In The International Journal of Computer Vision, Vol 1, Numero 2, pp 167-187, May 1987.
- [Der88] R. DERICHE and O.D. FAUGERAS: "2-D Curve Matching Using High Curvature Points: Application to Stereo Vision" 10th IAPR , Atlantic-City, New-Jersey, 18-23 June, 1990.
- [Dre82] L. DRESCHLER and H.H. NAGEL: "On the Selection of Critical Points and local Curvature Extrema of Region Boundaries for Interframe Matching", in International Conference on Pattern Recognition, 1982, pp 542-544.
- [Gui88] A. GUIDUCCI : "Corner Characterization by Differential Geometry Techniques", in Pattern Recognition Letters Vol 8 1988, pp 311-318.
- [Har87] C.G. HARRIS: "Determination of ego-motion from matched points", Proc. Alvey Vision Conf. Cambridge, UK, 1987.
- [Har88] C. HARRIS and M. STEPHENS : "A Combined Corner and Edge Detector", Proc 4th Alvey Vision Conf. Manchester August 1988 pp 189-192
- [Hua86] H.Z. HUA and Y. QUIAN : "A direct corner detection algorithm", in Proc. 8th ICPR October 1986, Paris. pp 853-855



- [Kit82] L. KITCHEN and A. ROSENFELD : "Gray-Level Corner Detection", in *Pattern Recognition Letters*, December 1982, pp 95-102.
- [Kru89] W.M. KRUEGER and K. PHILLIPS : "The Geometry of Differential Operators with Application to Image Processing", in *IEEE PAMI Vol11*, December 1989 pp 1252-1264
- [Lip69] M.M. LIPSCHUTZ : "Differential Geometry" McGraw-Hill, New York USA 1969
- [Mar80] D. MARR and E. Hildreth: "Theory of Edge Detection", In *Proc Roy Soc. London*, B207, 1980 pp 187-217
- [Mat88] S. WOLFRAM: " Mathematica : A system for doing mathematics by computer", in *Addison-Wesley Publishing Company*.
- [Med86] G. MEDIONI and Y. YASUMUTO : "Corner Detection and Curve Representation using cubic B-spline", *IEEE Int. Conf, Robotics and Automation* 1986, pp 764-769.
- [Mok86] F. MOKHTARIAN and A. MACKWORTH "Scale-based description and recognition of planar curves and 2D shapes", *IEEE PAMI Vol8 No 1* 1986 pp 34-43
- [Mor77] H.P. MORAVEC : "Towards Automatic Visual Obstacle Avoidance" *Proc Int. Joint Conf Artificial Intelligence* Cambridge, MA, USA August 1977 pp 584
- [Nag83a] H.H. NAGEL: "Displacement Vectors Derived from Second-Order Intensity Variations in Image Sequences", in *CVGIP Vol 21* 1983, pp 85-117.
- [Nag83b] H.H. NAGEL: "Constraints for the Estimation of Displacement Vector Fields from Image Sequences", in *International Joint Conference on Artif Intell*, Karlsruhe 1983, pp 156-160
- [Nob88] J.A. NOBLE : "Finding Corners", in *Image and Vision Computing*, Vol 6, may 1988 pp 121-128
- [Ran89] K. RANGARAJAN, M. SHAH and D.V. BRACKLE : "Optimal Corner Detector", in *CVGIP*, Vol 48, 1989, pp 230-245
- [Sha84] M.A. SHAH and R. JAIN: "Detecting Time-Varying Corners", in *CVGIP*, Vol28 1984 pp 345-355.
- [Tor86] V. TORRE and T.A. POGGIO: "On Edge Detection", in *IEEE PAMI*, Vol8, No2, March 1986, pp 147-163.

- [Zun83] O.A. ZUNIGA and R.M. HARALICK: " Corner detection using the facet model", in Proc. Conf. on Pattern Recognition Image Processing 1983 pp 30-37.

**ISSN 0249-6399**